



Available online at
ScienceDirect
 www.sciencedirect.com

Elsevier Masson France
EM|consulte
 www.em-consulte.com/en



Original article

Idarubicin-loaded folic acid conjugated magnetic nanoparticles as a targetable drug delivery system for breast cancer



Ufuk Gunduz^{a,b,*}, Tugba Keskin^a, Gulistan Tansik^a, Pelin Mutlu^{c,1}, Serap Yalcin^{d,1}, Gozde Unsoy^b, Arzu Yakar^e, Rouhollah Khodadust^b, Gungor Gunduz^f

^aMiddle East Technical University, Department of Biological Sciences, Ankara 06800, Turkey

^bMiddle East Technical University, Department of Biotechnology, Ankara 06800, Turkey

^cMiddle East Technical University, Central Laboratory, Molecular Biology and Biotechnology R&D Center, Ankara 06800, Turkey

^dAhi Evran University, Faculty of Engineering and Architecture, Kirsehir 40000, Turkey

^eAfyon Kocatepe University, Department of Chemical Engineering, Afyon 03200, Turkey

^fMiddle East Technical University, Department of Chemical Engineering, Ankara 06800, Turkey

ARTICLE INFO

Article history:

Received 22 July 2014

Accepted 7 August 2014

Keywords:

Idarubicin

Folic acid

Polyethylene glycol (PEG)

Magnetic nanoparticle

Drug delivery

MCF-7

ABSTRACT

Conventional cancer chemotherapies cannot differentiate between healthy and cancer cells, and lead to severe side effects and systemic toxicity. Another major problem is the drug resistance development before or during the treatment. In the last decades, different kinds of controlled drug delivery systems have been developed to overcome these shortcomings. The studies aim targeted drug delivery to tumor site. Magnetic nanoparticles (MNP) are potentially important in cancer treatment since they can be targeted to tumor site by an externally applied magnetic field. In this study, MNPs were synthesized, covered with biocompatible polyethylene glycol (PEG) and conjugated with folic acid. Then, anti-cancer drug idarubicin was loaded onto the nanoparticles. Shape, size, crystal and chemical structures, and magnetic properties of synthesized nanoparticles were characterized. The characterization of synthesized nanoparticles was performed by dynamic light scattering (DLS), Fourier transform-infrared spectroscopy (FT-IR), transmission electron microscopy (TEM), scanning electron microscopy (SEM) analyses. Internalization and accumulation of MNPs in MCF-7 cells were illustrated by light and confocal microscopy. Empty MNPs did not have any toxicity in the concentration ranges of 0–500 µg/mL on MCF-7 cells, while drug-loaded nanoparticles led to significant toxicity in a concentration-dependent manner. Besides, idarubicin-loaded MNPs exhibited higher toxicity compared to free idarubicin. The results are promising for improvement in cancer chemotherapy.

© 2014 Elsevier Masson SAS. All rights reserved.

1. Introduction

Chemotherapy is a systemic therapy using free drugs with poor biodistribution and targeting. Since conventional chemotherapeutics target only dividing cells without the ability of differentiation between cancer and healthy cells, their success is still questionable [1]. Targeted therapy agents have been developed to overcome the severe side effects of traditional chemotherapeutics on healthy cells. However, acquisition of drug resistance has also become a significant obstacle in targeted therapy [2]. Idarubicin, which is a synthetic analogue of daunorubicin, acts by intercalating between

DNA base pairs and inhibiting topoisomerase II [3,4]. Additionally, it induces free oxygen radicals leading to destruction of DNA and cell membrane [4]. Idarubicin differs from daunorubicin due to its lack of methoxy group at position 4 of the D ring of the aglycone [5,6]. This synthetic modification leads to high lipophilicity, better DNA binding, and greater cytotoxicity. However, despite its efficiency idarubicin possesses various side effects, like myelosuppression, neutropenia, induction of secondary tumours and disease relapse due to multiple drug resistance (MDR). This necessitates its formulation into novel nanosized drug delivery vehicles to exploit its benefits in minimizing its systemic exposure and thus reducing non-specific toxicity, but retaining its efficacy at the tumour site [7]. The polymer coated magnetic nanoparticles have been widely studied as drug vectors, based on their lack of toxicity, biodegradability, good biocompatibility, and absorption [8–10]. General structure of magnetic nanoparticles (MNPs) is

* Corresponding author. Biological Sciences, METU, Ankara 06800, Turkey.

Tel.: +90 312 210 51 84.

E-mail address: ufukg@metu.edu.tr (U. Gunduz).

¹ Co-Authors equally contributed for this manuscript.

composed of an inner magnetic core and an outer polymeric shell. Magnetic core is usually a magnetite (Fe_3O_4) or maghemite (Fe_2O_3). It is covered with a polymeric shell, which renders MNPs biocompatibility, prevents their agglomeration and functions as drug reservoir [11]. Different types of polymers and molecules are used for covering surfaces of naked magnetic nanoparticles to stabilize them and for further biological applications. Starch, dextran, polyethylene glycol, fatty acids, polyvinyl alcohol, polyacrylic acid, poly lactides, gelatin and chitosan are some of the examples of widely used coating materials for different purposes [12]. PEG is one of the mostly used synthetic polymers to cover MNP. It gives MNP a hydrophilic surface and minimizes agglomeration. Thus, PEG coating enhances the circulation time of MNPs by reducing their phagocytosis by macrophages [13]. One of the most important limitations of cancer therapy is the lack of specificity of anti-cancer drug delivery. There is an increasing demand for the improvement of the effectual delivery of drugs to the targeted tumor site. There are distinctive features between cancer and healthy cells, which can be, used as preferred targets in the treatment. Cancer cells often express several proteins on the cell surface in greater amounts than the normal cells. One of the most preferable drug carrier models is multifunctional nanocarriers that comprise a high payload of drugs and targeting moieties, which bind to specific proteins that are overexpressed in cancer cells [14–16].

Folic acid receptors (FR) are found to be overexpressed on different types of cancer cells including breast cancer [17]. Normal cells do not express FR or it locates on apical surface of polarized epithelia where drugs cannot reach [18]. Besides, while only reduced folate can be transported in healthy cells, cancer cells are able to transport folate conjugates by FR via receptor mediated endocytosis. By this mechanism, folic acid covered and drug-loaded nanoparticles can overcome drug resistance caused by P-glycoprotein efflux pumps [2]. The natural characteristics of folic acid and folic acid receptors on cancer cells make them very efficient agents for drug targeting being ameliorate the severe side effects of free drugs and overcome drug resistance [18].

The aim of this study is synthesis and characterization of PEG coated, folic acid conjugated, idarubicin-loaded magnetic nanoparticles; investigating their drug release properties, internalization, and antiproliferative effects on MCF-7 cells for potential utilization as a targetable drug delivery system in breast cancer treatment.

2. Material and methods

2.1. Materials

Iron (II) chloride tetrahydrate ($\text{FeCl}_2 \cdot 4\text{H}_2\text{O}$), iron (III) chloride hexahydrate ($\text{FeCl}_3 \cdot 6\text{H}_2\text{O}$), oleic acid, polyethylene monooleate, folic acid, dicyclohexyl carbodiimide (DCC) and dimethylsulfoxide (DMSO) were purchased from Sigma–Aldrich (USA). Ammonium hydroxide solution (NH_4OH) was obtained from Merck (Germany). Dimethylsulfoxide (cell culture grade) was obtained from Appli-chem (Germany). MCF-7 monolayer type human epithelial breast adenocarcinoma cell line was provided from Food and Mouth Diseases Institute (Ankara), RPMI 1640 medium [(1×), 2.0 g/L NaHCO_3 stable glutamine], fetal bovine serum were obtained from Biochrom Ag. (Germany). Trypsin–EDTA solution (0.25% Trypsin–EDTA), gentamycin sulphate (50 mg/mL as base), trypan blue solution (0.5%), cell proliferation kit (XTT assay) were obtained from Biological Industries, Kibbutz Beit Haemek (Israel).

2.2. Preparation of MNPs

Magnetic iron oxide (Fe_3O_4) nanoparticles were synthesized by the co-precipitation of Fe(II) and Fe(III) salts at 1:2 ratio in 150 mL

deionized water within a five-necked glass balloon [19,20]. It is vigorously stirred in the presence of nitrogen (N_2) gas at 90 °C. Ammonium hydroxide (NH_4OH) is added to the system dropwise. The process ends by washing with deionized H_2O until the solution pH is 9.0.

2.3. Preparation of oleic acid coated MNPs

Oleic acid was directly added into synthesis system with iron oxide nanoparticles and stirred for 1 h by mechanical stirrer. Particles were washed 3 times with acetone and ethanol to get rid of excess amount of oleic acid and labeled as OA–MNP.

2.4. Functionalization of MNPs with PEG

Oleic acid conjugated PEG monooleate was used as polymeric surfactant. It was hypothesized that the oleate part of PEG monooleate would adsorb onto oleic acid coating on the iron oxide core. Hence, PEG could form an exterior surface layer that renders MNP hydrophilicity. After the synthesis of oleic acid coated MNPs, the temperature of the system was decreased to room temperature, and the aqueous solution of PEG monooleate was added to system and the stirring was continued for an additional 24 h at room temperature. PEG coated MNP obtained by this method was labeled as PEG–MNP.

2.5. Modification of MNPs with folic acid

Folic acid needs the activation of its carboxyl group with dicyclohexyl carbodiimide (DCC) to conjugate to surface polymer [21]. Folic acid and DCC with 1:1 ratio were added in dimethyl sulfoxide (DMSO) and stirred for 2 h. PEG–MNP sample was added into system and continuously stirred for 2 h under a nitrogen atmosphere. After washing of the nanoparticles with dH_2O , they were freeze-dried for one night. The sample stirred for 2 h labelled as FA–PEG–MNP.

2.6. Characterization of magnetic nanoparticles

The characterization of synthesized nanoparticles was performed by dynamic light scattering (DLS), transmission electron microscopy (TEM) and Fourier transform–infrared spectroscopy (FT–IR).

2.7. Light microscopy observation of FA–PEG–MNP treated cells and Prussian blue staining

MCF-7/S cells were seeded in 6-well plate (25,000 cells/well) and incubated with FA–PEG–MNPs (500 $\mu\text{g}/\text{mL}$). After 48 h of incubation, cells were washed with PBS and observed under light microscopy (40×) (Olympus, USA). Prussian blue staining kit (Sigma–Aldrich) was also used to show the cell uptake of FA–PEG–MNPs. After 8 h incubation period of MCF-7 cells with FA–PEG–MNPs (200 $\mu\text{g}/\text{mL}$), Prussian blue staining was performed according to the manufacturer's instructions. Accumulation of nanoparticles was visualized under light microscopy (40×) (Olympus, USA).

2.8. Idarubicin loading on FA–PEG–MNPs

Idarubicin (IDA) was prepared as stock solution, which dissolved in DMSO. FA–PEG–MNPs (1 mg) and idarubicin in the range of 30–400 μM (in 2 mL PBS) were rotated at 95 rpm for 24 h while being protected from light. After the incubation period, IDA-loaded FA–PEG–MNPs were separated by magnetic separation and the idarubicin loading efficiency was quantified by measuring the

absorbance values at 484 nm by a Shimadzu UV-spectrophotometer (Columbia, USA).

2.9. Release of idarubicin from FA-PEG-MNPs

The release of idarubicin from MNPs loaded with 1 mg was analyzed in PBS buffer at pH 5.4 and pH 7.4 up to 72 h. The amount of released idarubicin was determined by measuring the absorbance of the solution at 484 nm by a Shimadzu UV-spectrophotometer (Columbia, USA).

2.10. Confocal microscopy observation of free idarubicin and IDA-MNP treated cells

The internalization of idarubicin and idarubicin-loaded nanoparticles were shown by confocal microscopy. Autoclaved coverslips (Marienfeld, Germany) were placed into the wells of a 6-well plate. MCF-7 cells were seeded onto the coverslips and transfected in 6-well format. After 4 h, cells were washed three times with PBS. After treatment cells were fixed with 2% (w/v) paraformaldehyde in PBS. The coverslips were wet-mounted on microscope slides and observed under the Zeiss LSM 510 confocal laser scanning microscope.

2.11. Cell proliferation assay

XTT cell proliferation assay was carried out to understand whether synthesized naked MNPs, PEG-MNPs and idarubicin-loaded FA-PEG-MNPs have a cytotoxic effect on MCF-7 cells. The kit based on the idea that metabolically active cells can reduce XTT (2,3-bis (2-methoxy-4-nitro-5-sulphophenyl)-2H-tetrazolium-5-carboxanilide) tetrazolium salt to orange colored, water soluble formazan products by mitochondrial enzymes which are inactivated after cell death. In brief, cells were seeded to 96-well microliter plates (Greiner) at a concentration of 5.0×10^4 cells/well and incubated for 72 h in medium containing horizontal dilutions of either each MNP or free Idarubicin. In each plate, assay was performed with a column of blank medium control and a cell control columns. Then, XTT reagent was added and soluble product was measured at 492 nm with a Spectromax 340 96-well plate reader (Molecular Devices, USA).

2.12. Statistical analysis

All data representative of three independent experiments, each run in triplicates and expressed as mean standard error of means (SEM). Graphpad Prism 5 Demo Software (GraphPad Software, Inc. USA) was used and One-way ANOVA test was carried out for statistical analysis.

3. Results

3.1. Dynamic light scattering (DLS)

The hydrodynamic sizes of uncoated and oleic acid coated MNPs were determined with DLS measurements. The average sizes of uncoated MNPs and OA-MNPs were found as 221 nm and 131 nm, respectively (Figs. 1 and 2).

3.2. Transmission electron microscopy (TEM)

Shapes and sizes of FA conjugated PEG coated MNPs were analyzed by TEM. In Fig. 3, shape and morphology of FA-PEG-MNP nanoparticles are seen regular and spherical. Their sizes were between 10–40 nm approximately.

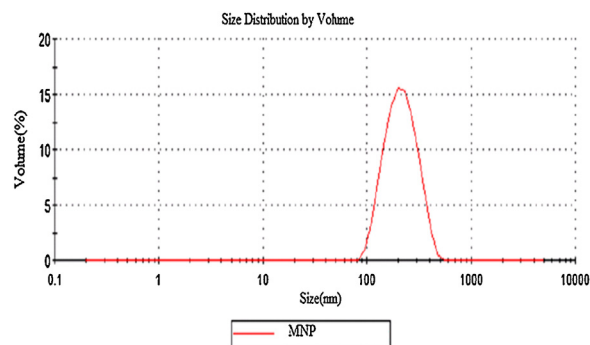


Fig. 1. Particle size distribution of uncoated MNPs.

3.3. Fourier transform-infrared (FT-IR) spectroscopy

Oleic acid coated MNP, PEG coated MNP and folic acid functionalized MNP were characterized with FT-IR spectroscopy. FT-IR spectrum of this nanoparticles is given in Fig. 4. In Fig. 4, different and similar peaks OA-MNP, PEG-MNP and FA-PEG-MNP are seen. All three curves revealed the characteristic peak of oleic acid around 2924 cm^{-1} , 2854 cm^{-1} and 3005 cm^{-1} belonging to asymmetric, symmetric CH_2 stretching and C-H stretching bond in C=C-H. Additionally, Fe-O stretching of Fe_3O_4 was observed around 580 cm^{-1} in the curves of all samples. Peaks indicating the presence of PEG or folic acid were indicated with arrow. Compared to OA-MNP, additional peaks around 1109 and 945 cm^{-1} were observed in the curve of PEG-MNP and FA-PEG-MNP attributed to C-O-C stretching and bending of C-H of polyethylene glycol. In the adsorption spectra of FA-PEG-MNP, new peaks at 1696 cm^{-1} and 1627 cm^{-1} were derived from mainly folic acid.

3.4. Light microscopy observation of FA-PEG-MNP treated cells and Prussian blue staining

To visualize the uptake of FA-PEG-MNPs into MCF-7 cells, light microscopy examination was carried out. In Fig. 5a light microscopy image of MCF-7 cells which are not treated with FA-PEG-MNPs is provided. On the other hand, in Fig. 5b, it was shown that after the treatment of MCF-7 cells with FA-PEG-MNP, the nanoparticles were taken into the cell and gathered around nuclear membrane but could not enter into the nucleus.

Prussian blue staining method was used in order to examine the uptake of FA-PEG-MNPs into the cells. In this method, MCF-7 cells were stained with Prussian blue 8 h after the treatment of nanoparticles and visualized under the light microscope. At the end of the staining procedure, light pink coloring of cytoplasm,

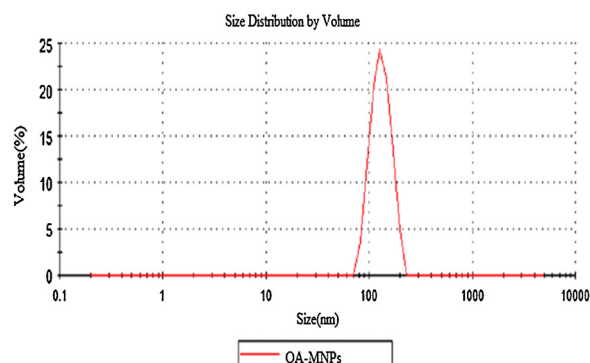


Fig. 2. Particle size distribution of OA-MNPs.

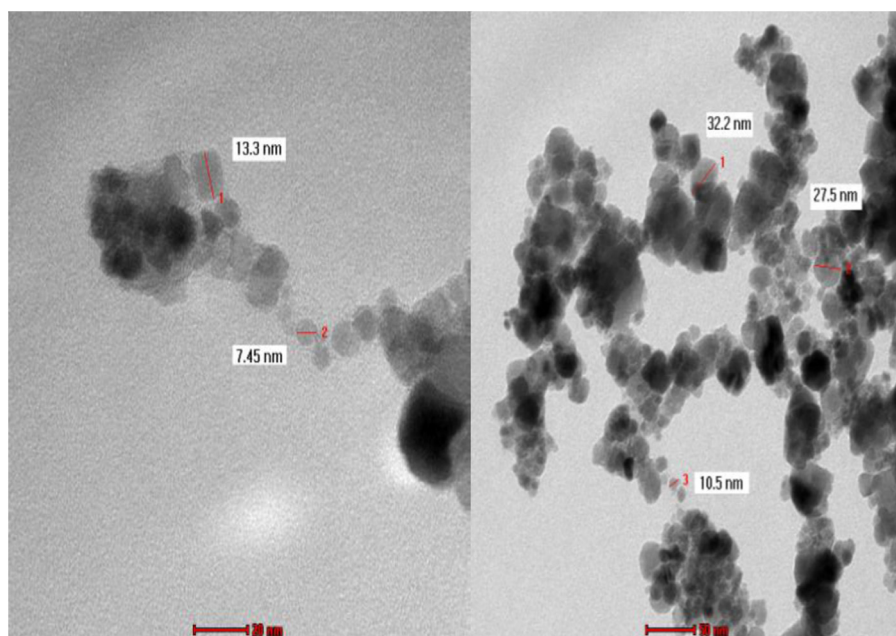


Fig. 3. TEM images of FA-PEG-MNP.

dark pink coloring of nucleus and blue coloring of iron core of the molecules is expected. Fig. 6 shows the light microscopy images of the FA-PEG-MNP treated and untreated MCF-7 cells after Prussian blue iron staining.

3.5. Idarubicin loading efficiencies to FA-PEG-MNPs

Loading efficiencies were tested in PBS buffer with different drug concentrations (30, 50, 250, 300, 400 μM) and 1 mg FA-PEG-MNPs. To find maximum drug loading capacity on nanoparticles, Idarubicin concentration gradually increased up to 400 μM , however, the loading efficiency started to decrease at 300 μM . The most efficient drug conjugation concentration was obtained as 250 μM ($36.1 \pm 3.4\%$) (Fig. 7). The loading efficiency of the highest drug concentration (400 μM) was found as $14.1 \pm 2.8\%$.

Drug-loaded nanoparticles (IDA-MNP), free idarubicin (IDA) and bare nanoparticles (MNP) was analysed by UV-spectrophotometer at 350–800 nm. The highest absorbance values of idarubicin and drug-loaded nanoparticles was found at 484 nm. According to these results, it can be concluded that idarubicin was successfully loaded onto the nanoparticles (Fig. 8).

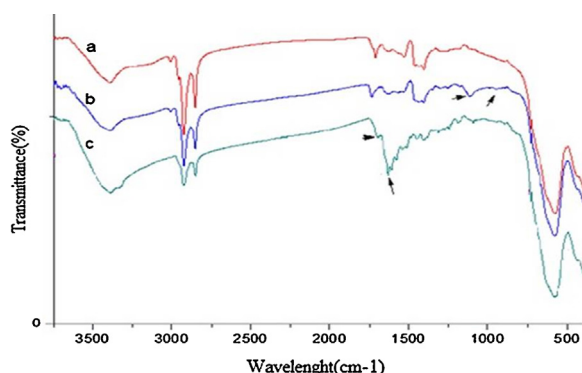


Fig. 4. FT-IR spectra of OA-MNP (a), PEG-MNP (b), FA-PEG-MNP (c).

3.6. Release of idarubicin from FA-PEG-MNPs

Idarubicin release studies were performed in acetate buffers having pH 5.4 and 7.0. The release profiles of IDA-MNPs at pH 5.4 and pH 7.0 are given in Fig. 9. The release studies were continued up to 72 h. Most of the drug (80%) was released within first 12 h at pH 5.4, whereas nearly 60% of the drug was released at pH 7.0 within this time interval (Fig. 9). The release of the drug becomes slower after 24 h and 90% of the drug was released up to 72 h.

3.7. Cellular internalization of idarubicin-loaded magnetic nanoparticles

Cellular uptake of free idarubicin and idarubicin-loaded nanoparticles (IDA-MNP) was demonstrated by confocal laser scanning microscopy (Fig. 10). The images were used to compare the intracellular accumulation of IDA-MNPs and free idarubicin in MCF-7 cells. Fig. 10 indicates that IDA-MNPs were successfully internalized by MCF-7 cells.

Fluorescence intensities of free idarubicin and IDA-MNPs inside the cells at the end of 4 h incubation period were compared in Fig. 11. IDA-MNPs accumulated nearly more than 90-fold inside the cells in comparison to free idarubicin.

3.8. Cytotoxicity of idarubicin-loaded magnetic nanoparticles

To assess the cytotoxicities of synthesized MNPs, PEG-MNPs and IDA-MNPs, cell proliferation assays were performed. MCF-7 cells incubated with different concentrations of naked MNPs and PEG-MNPs (0–500 $\mu\text{g}/\text{mL}$) did not exhibit a dramatic cell death. To quantify the cytotoxic effects of IDA-MNPs, inhibitory concentration 50 (IC_{50}) values were calculated, which show the toxic dose. It was found that the released idarubicin from the MNPs has the capacity to kill the MCF-7 cells efficiently (Fig. 12). According to the XTT results, IC_{50} value of 2.48 μM free idarubicin decreased to 1.25 μM when idarubicin was given as loaded on FA-PEG-MNPs to MCF-7 cells. Idarubicin-loaded MNPs were about 2-fold more cytotoxic as compared to free drug on MCF-7 cell line *in vitro*.

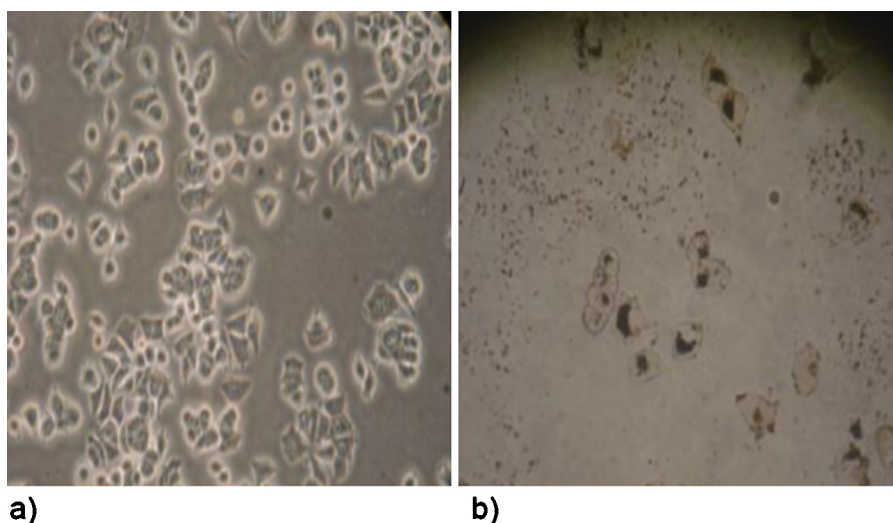


Fig. 5. Light microscopy images (a) FA-PEG-MNP untreated MCF-7 cells (b) FA-PEG-MNP treated MCF-7 cells.

4. Discussion

The diversity and efficiency of carrier systems for drug targeting and controlled drug release applications are critical to eliminate the chemotherapy-induced side effects. Especially by the improvements in the synthesis of magnetic nanoparticles, which can be targeted to the tumor site under magnetic field, such progress has been made in research. Polymer coated magnetic nanoparticles have been proven for their efficiency to deliver anti-cancer agents due to their ability to transport large quantities of therapeutic molecules, targeted in tumor site, prolonged circulation time and subsequent slow release of the drug [7,22]. Polymeric materials, such as PEG, proteins, polysaccharides, polylactic acids, poloxamines and poloxamers that are used for

coating MNPs, have desirable attributes like enhanced biocompatibility, biodegradability and cellular uptake [7,23–25]. In addition, nanoparticles with more hydrophobic surface will preferentially be taken up by liver and presentation of more hydrophilic surface is desired [26]. Therefore, insertion of hydrophilic PEG groups on the surface of nanoparticle is a common strategy [27].

In this study, PEG coated and folic acid conjugated magnetic nanoparticles were synthesized and loaded with idarubicin. The size of the nanoparticles was in the range of 10–40 nm, which is the suitable size for biomedical applications [28]. Particle size is a very important parameter since nanoparticles with large size will usually be taken up by reticuloendothelial system (RES) and particles with size less than 100 nm in diameter with a uniform size distribution are suitable for tumor targeting [29–32].

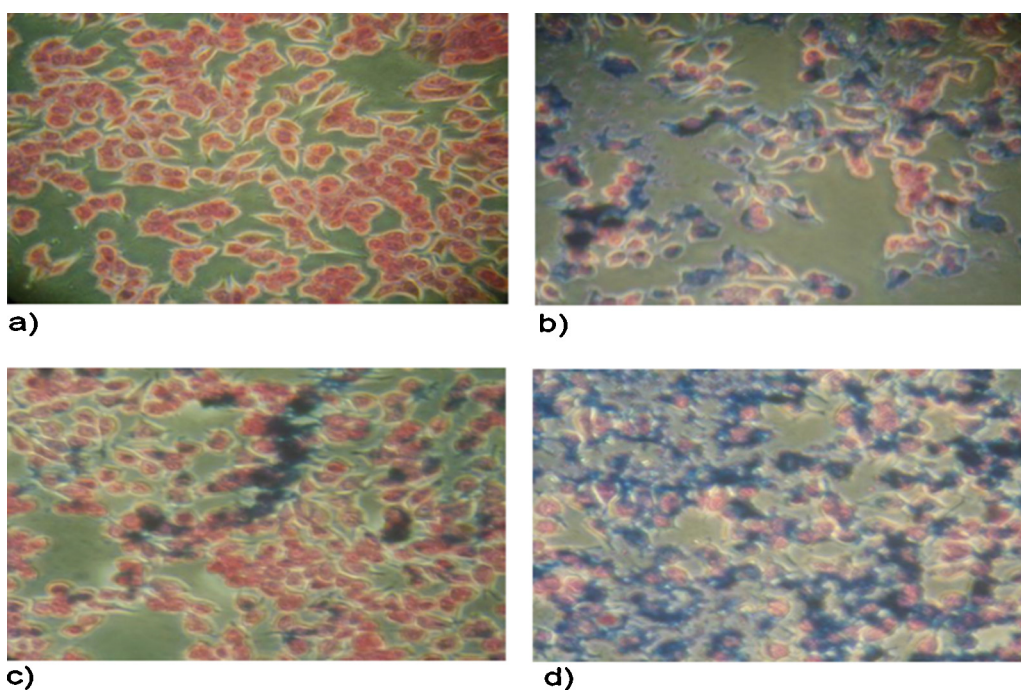


Fig. 6. Light microscopy images of stained MCF-7 cells that are treated with FA-PEG-MNPs. a: control group: FA-PEG-MNP untreated MCF-7 cells; b: MCF-7 cells treated with FA-PEG-MNP and have not been subjected to magnetic field; c: MCF-7 cells treated with FA-PEG-MNP, have been subjected to magnetic field and away from the magnet; d: MCF-7 cells treated with FA-PEG-MNP, have been subjected to magnetic field and close to the magnet.

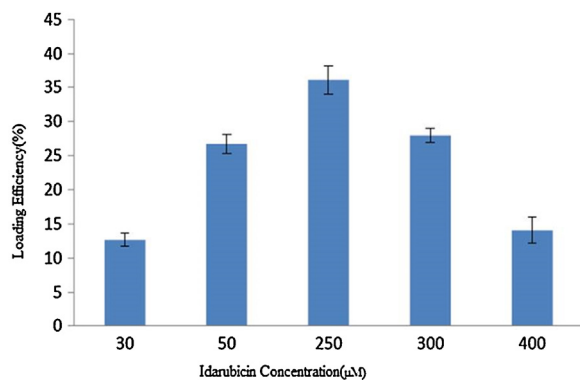


Fig. 7. Loading efficiencies of idarubicin onto FA-PEG-MNPs.

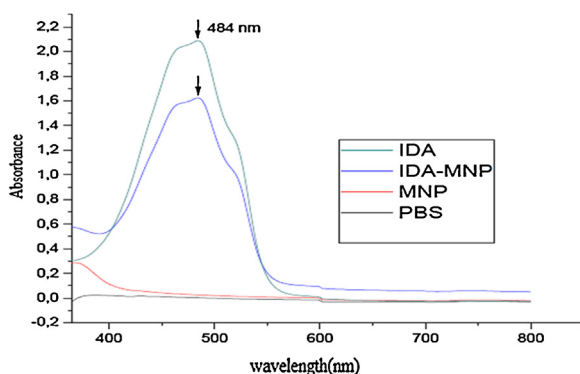


Fig. 8. UV absorbance spectra of free IDA, IDA-MNP, naked MNP and PBS.

Light microscopy images indicate the successful cellular uptake of FA-PEG-MNPs. In order to investigate the effect of external magnetic field on MCF-7 cells incubated with nanoparticles, a powerful magnet (Nd-Fe-B) was located at the right bottom part of the culture dish. As expected, the accumulation of FA-PEG-MNPs was more in the cells, which are close to the magnet site. According to this result, it can be concluded that these nanoparticles can be targeted to the desired location in vitro conditions. Also, this tends to be a guide for in vivo drug targeting studies.

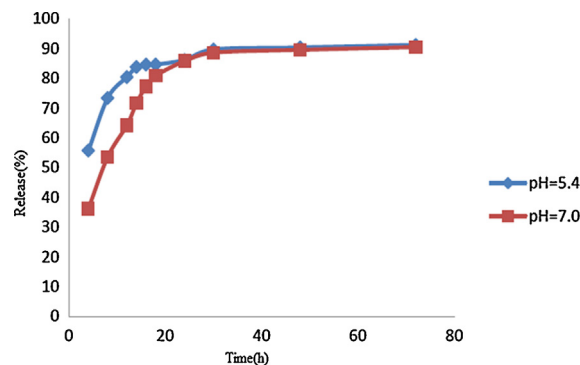


Fig. 9. Idarubicin release ratio from FA-PEG-MNPs at pH 5.4 and pH 7.0.

The most efficient drug incorporation ratio to FA-PEG-MNPs was approximately 36% for 250 μM idarubicin, while 90% of the drug was released within 72 h at pH 7.0. The release efficiencies of IDA-MNPs were investigated at acetate buffers with two different pH values of 5.4 and 7.0. The release of the drug at pH 7.0 is slower compared to pH 5.4 within 12 h. It is known that the pH of the tumor microenvironment is low (pH 4.0–5.5) due to the high anaerobic glucose metabolism of cancer cells [33,34]. Due to the drug release acceleration with the decrease in pH, these nanoparticles are expected to have an effective drug release in the tumor microenvironment.

The results of the cytotoxicity analysis of the unloaded MNPs exhibited no significant toxicity at the highest concentration tested. Although, the idarubicin loading efficiency on FA-PEG-MNPs is lower with respect to propyl starch [35] and solid lipid [7] nanoparticles, there is statistically significant difference in cytotoxicity of IDA-MNPs compared to free IDA on MCF-7 cells.

The internalization of free idarubicin and idarubicin-loaded magnetic nanoparticles were shown by confocal microscopy. It was visualized that IDA-MNPs were successfully internalized by MCF-7 cells and accumulated more than free idarubicin inside the cells. This can be due to the differences of the internalization mechanism of free idarubicin and IDA-MNPs. Free idarubicin diffuses through the cell membrane and cannot accumulate much into the cells due to the ATP-dependent efflux pumps on the cell membrane [36]. However, FA-PEG-MNPs are taken by endocytosis

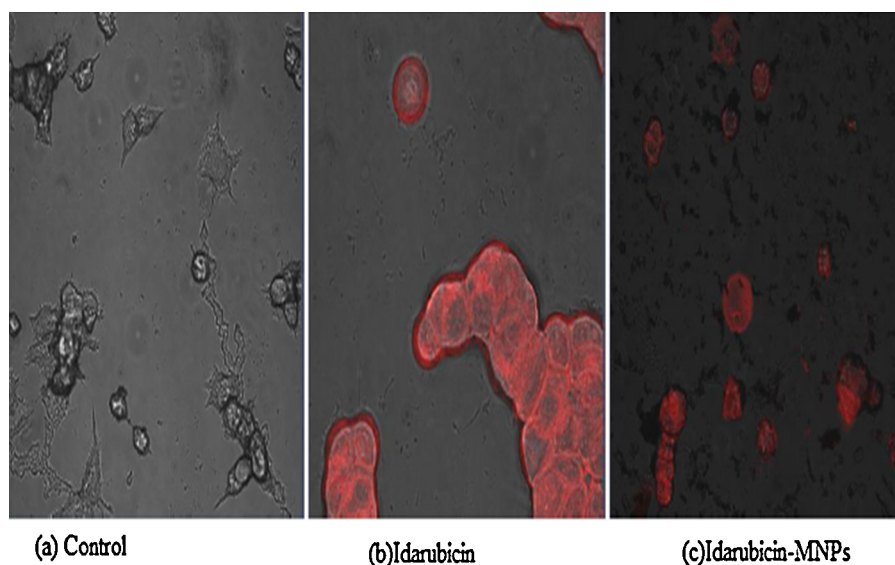


Fig. 10. Confocal microscopy images of free idarubicin and IDA-MNP treated MCF-7 cells. a: control group: MCF-7 cells; b: free idarubicin treated MCF-7 cells; c: IDA-MNP treated MCF-7 cells.

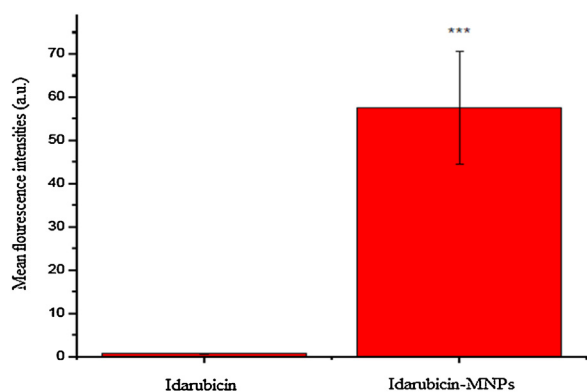


Fig. 11. Mean fluorescence intensities of free IDA and IDA-MNP treated MCF-7 cells at the end of 4-h incubation period.

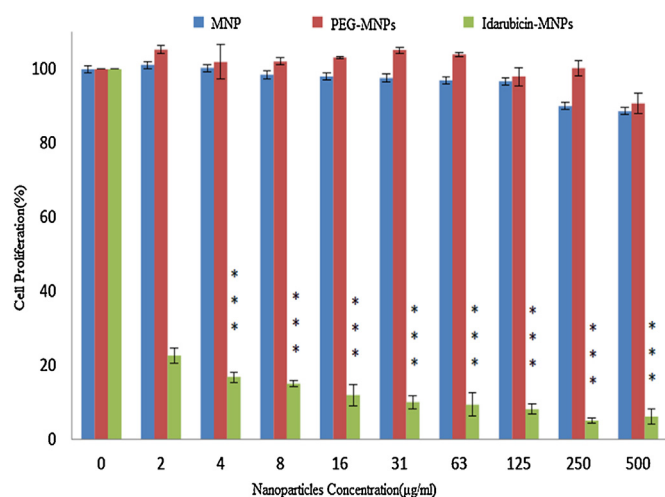


Fig. 12. The cytotoxic effect of MNPs, PEG-MNPs and IDA-MNPs on MCF-7 cells (72 h) ($P < 0.05$).

and when idarubicin is loaded to these nanoparticles, it can escape from the efflux pumps and can accumulate in the cells. IDA-loaded nanoparticles have also been formulated to address P-gp-mediated multidrug resistance (MDR) by several other research groups. However, IDA-loaded liposomes and solid lipid nanoparticles showed comparable cytotoxicity with free IDA in these studies [7,37]. Our findings have indicated that higher cytotoxicities can be obtained by idarubicin when loaded onto our nanoparticles. It can be concluded that idarubicin-loaded FA-PEG-MNPs are superior to lipid coated nanoparticles in terms of the cytotoxic effect on MCF-7 breast cancer cell line. In addition to their targetable characteristics, IDA-MNPs being conjugated with folic acid can also be chemically targeted to the different types of cancer cells which have folic acid receptors on their cellular membrane.

5. Conclusion

In conclusion, idarubicin-loaded, folic acid conjugated magnetic nanoparticles, which have desired shape and sizes, chemical and magnetic properties were synthesized for biomedical applications. Drug loading and release efficiencies of these nanoparticles were investigated. Internalization into MCF-7 cells and targeting ability under magnetic field were determined in vitro. IDA-MNPs were found more cytotoxic on MCF-7 cells when compared to free idarubicin. The results of this study can provide new insights to the

development of new drug delivery systems. The biocompatibility, systemic toxicity, accumulation in different tissues and their metabolic route of these nanoparticles remain to be determined by in vivo studies.

Acknowledgement

This study was supported by TUBITAK (TBAG-109T949).

References

- [1] Van Vlerken LE, Amiji MM. Multi-functional polymeric nanoparticles for tumour-targeted drug delivery. *Expert Opin Drug Deliv* 2006;3:205–16.
- [2] Cho K, Wang X, Nie S, Chen ZG, Shin DM. Therapeutic nanoparticles for drug delivery in cancer. *Clin Cancer Res* 2008;14:1310–6.
- [3] Takimoto CH, Calvo E. Principles of oncologic pharmacotherapy. In: Pazdur R, Wagman LD, Camphausen KA, Hoskins WJ, editors. *Cancer Management: A Multidisciplinary Approach*. Norwalk: UBM Medica; 2008.
- [4] Minotti G, Menna P, Salvatorelli E, Cairo G, Gianni L. Anthracyclines: molecular advances and pharmacologic developments in antitumor activity and cardiotoxicity. *Pharmacol Rev* 2004;56:185–229.
- [5] Gubernator J, Chwastek G, Korycińska M, Stasiuk M, Gryniewicz G, Lewrick F, et al. The encapsulation of idarubicin within liposomes using the novel EDTA ion gradient method ensures improved drug retention in vitro and in vivo. *J Control Release* 2010;146:68–75.
- [6] Hande KR. Topoisomerase II inhibitors. *Update Cancer Ther* 2008;3:13–26.
- [7] Ma P, Dong X, Swadley CL, Gupte A, Leggas M, Ledebur HC, et al. Development of idarubicin and doxorubicin solid lipid nanoparticles to overcome Pgp-mediated multiple drug resistance in leukemia. *J Biomed Nanotechnol* 2009;5:151–61.
- [8] Hamman JH. Chitosan based polyelectrolyte complexes as potential carrier materials in drug delivery systems. *Mar Drugs* 2010;8:1305–22.
- [9] Arulmozhi V, Pandian K, Mirunalini S. Ellagic acid encapsulated chitosan nanoparticles for drug delivery system in human oral cancer cell line (KB). *Colloids Surf B Biointerf* 2013;110:313–20.
- [10] Javid A, Ahmadian S, Saboury AA, Kalantar SM, Rezaei-Zarchi S. Chitosan coated superparamagnetic iron oxide nanoparticles for doxorubicin delivery: synthesis and anticancer effect against human ovarian cancer cells. *Chem Biol Drug Des* 2013;82:296–306.
- [11] McBain SC, Yiu HHP, Dobson J. Magnetic nanoparticles for gene and drug delivery. *Int J Nanomedicine* 2008;3:169–80.
- [12] Gupta AK, Gupta M. Synthesis and surface engineering of iron oxide nanoparticles for biomedical applications. *Biomaterials* 2005;26:3995–4021.
- [13] Sun C, Lee JSH, Zhang M. Magnetic nanoparticles in MR imaging and drug delivery. *Adv Drug Deliv Rev* 2008;60:1252–65.
- [14] Moghimi SM, Peer D, Langer R. Reshaping the future of nanopharmaceuticals: ad iudicium. *ACS Nano* 2011;5:8454–8.
- [15] Xiao Z, Levy-Nissenbaum E, Alexis F, Lupták A, Tpey BA, Chan JM, et al. Engineering of targeted nanoparticles for cancer therapy using internalizing aptamers isolated by cell-uptake selection. *ACS Nano* 2012;6:696–704.
- [16] Perfezou M, Turner A, Merkoçi A. Cancer detection using nanoparticle-based sensors. *Chem Soc Rev* 2012;41:2606–22.
- [17] Byrne JD, Betancourt T, Peppas LB. Active targeting schemes for nanoparticle systems in cancer therapeutics. *Adv Drug Deliv Rev* 2008;60:1615–26.
- [18] Lu Y, Low PS. Folate-mediated delivery of macromolecular anticancer therapeutic agents. *Adv Drug Deliv Rev* 2002;54:675–93.
- [19] Liu X, Kaminski M, Guan Y, Chen H, Liu H, Rosengart AJ. Preparation and characterization of hydrophobic superparamagnetic magnetite gel. *J Magn Mater* 2006;306:248–53.
- [20] Yallapu MM, Foy SP, Jain TK, Labhasetwar V. PEG-functionalized magnetic nanoparticles for drug delivery and magnetic resonance imaging applications. *Pharm Res* 2010;27:2283–95.
- [21] Zhang J, Rana S, Sriavastava RS, Misra RDK. On the chemical synthesis and drug delivery response of folate receptor-activated, polyethylene glycol-functionalized magnetite nanoparticles. *Acta Biomater* 2008;4:40–8.
- [22] Kultarne SA, Low PS. Targeting of nanoparticles: folate receptor. In: Grobmyer SR, Moudgil BM, editors. *Methods in Molecular Biology*. New York: Humana Press, Springer Science+Business Media, LLC; 2010. p. 249–65.
- [23] Ringsdorf H. Structure and properties of pharmacologically active polymers. *J Polym Sci Polym Symp* 1975;51:135–53.
- [24] Moghimi SM, Hunter AC. Poloxamers and poloxamines in nanoparticles engineering and experimental medicine. *Trends Biotechnol* 2000;18:412–20.
- [25] Park EK, Lee SB, Lee YM. Preparation and characterization of methoxy-poly(ethylene glycol)/poly(epsilon-caprolactone) amphiphilic block copolymeric nanospheres for tumor-specific folate-mediated targeting of anticancer drugs. *Biomaterials* 2005;26:1053–61.
- [26] Storm G, Belliot SO, Daemen T, Lasic D. Surface modification of nanoparticles to oppose uptake by the mononuclear phagocyte system. *Adv Drug Deliv Rev* 1995;17:31–48.
- [27] Oyewumi MO, Yokel RA, Jay M, Coakley T, Mumper RJ. Comparison of cell uptake, biodistribution and tumor retention of folate-coated and PEG-coated gadolinium nanoparticles in tumor-bearing mice. *J Control Release* 2004;95:613–26.

- [28] Brannon-Peppas L, Blanchette JO. Nanoparticle and targeted systems for cancer therapy. *Adv Drug Deliv Rev* 2004;56:1649–59.
- [29] Peppas LB, Blanchette JO. Nanoparticle and targeted systems for cancer therapy. *Adv Drug Deliv Rev* 2004;56:1649–59.
- [30] Unsoy G, Khodadust R, Yalcin S, Mutlu P, Gunduz U. Synthesis of doxorubicin loaded magnetic chitosan nanoparticles for pH responsive targeted drug delivery. *Eur J Pharm Sci* 2014;62:243–50.
- [31] Khodadust R, Mutlu P, Yalcin S, Unsoy G, Gunduz U. Doxorubicin loading, release, and stability of polyamidoamine dendrimer-coated magnetic nanoparticles. *J Pharm Sci* 2013;102:1825–35.
- [32] Yalcin S, Erkan M, Unsoy G, Parsian M, Kleeff J, Gunduz U. Effect of gemcitabine and retinoic acid loaded PAMAM dendrimer-coated magnetic nanoparticles on pancreatic cancer and stellate cell lines. *Biomed Pharmacother* 2014. <http://dx.doi.org/10.1016/j.biopha.2014.07.003>.
- [33] Engin K, Leeper DB, Cater JR, Thistlethwaite AJ, Tupchong L, McFarlane JD. Extracellular pH distribution in human tumors. *Int J Hyperther* 1995;11:211–6.
- [34] Ojugo ASE, Mesheehy PMJ, McIntyre DJO, McCoy C, Stubbs M, Leach MO, et al. Measurement of the extracellular pH of solid tumors in mice by magnetic resonance spectroscopy: a comparison of exogenous ¹⁹F and ³¹P probes. *NMR Biomed* 1999;12:495–504.
- [35] Jain R, Dandekar P, Loretz B, Melero A, Stauner T, Wenz G, Koch M, et al. Enhanced cellular delivery of idarubicin by surface modification of propyl starch nanoparticles employing pteric acid conjugated polyvinyl alcohol. *Int J Pharm* 2011;420:147–55.
- [36] Stein WD. Kinetics of the multidrug transporter (P-glycoprotein) and its reversal. *Physiol Rev* 1997;77:545–90.
- [37] Santos ND, Waterhouse D, Masin D, Tardi PG, Karlsson G, Edwards K, et al. Substantial increases in idarubicin plasma concentration by liposome encapsulation mediates improved antitumor activity. *J Control Release* 2005;105:89–105.